PAPD5-mediated 3′ adenylation and subsequent degradation of miR-21 is disrupted in proliferative disease

Joost Boele[a,b], Helena Persson[c,1], Jay W. Shin[a,d], Yuri Ishizu[a,d], Inga S. Newie[e], Rolf Søkilde[e], Shannon M. Hawkins[f], Cristian Coarfa[g], Kazuhiro Ikeda[h], Ken-ichi Takayama[i,j], Kuniko Horie-Inoue[h], Yoshinari Ando[a,k], A. Maxwell Burroughs[a,l], Chihiro Sasaki[a], Chizuru Suzuki[a], Mizuho Sakai[a,d], Shintaro Aoki[a,d], Ayumi Ogawa[a], Akira Hasegawa[a,d], Marina Lizio[a,d], Kaoru Kaida[a,d], Bas Teusink[b], Piero Carninci[a,d], Harukazu Suzuki[a,d], Satoshi Inoue[h,i,j], Preethi H. Gunaratne[m,n], Carlos Rovira[e], Yoshihide Hayashizaki[a,o], and Michiel J. L. de Hoon[a,d,2]

[a]RIKEN Omics Science Center, Yokohama, Kanagawa 230-0045, Japan; [b]Department of Systems Bioinformatics, Amsterdam Institute for Molecules, Medicines and Systems, VU University Amsterdam, 1081 HV, Amsterdam, The Netherlands; [c]Department of Biosciences and Nutrition, Karolinska Institutet, SE-141 83 Huddinge, Sweden; [d]Division of Genomic Technologies, RIKEN Center for Life Science Technologies, Yokohama, Kanagawa 230-0045, Japan; [e]Division of Oncology, Department of Clinical Sciences, Lund University Cancer Center/Medicon Village, SE-223 81 Lund, Sweden; [f]Department of Obstetrics and Gynecology and Center for Reproductive Medicine, [g]Department of Molecular and Cellular Biology, and [m]Department of Pathology and Immunology, Baylor College of Medicine, Houston, TX 77030; [h]Division of Gene Regulation and Signal Transduction, Research Center for Genomic Medicine, Saitama Medical University, Saitama 350-1241, Japan; Departments of [i]Anti-Aging Medicine and [j]Geriatric Medicine, Graduate School of Medicine, University of Tokyo, Bunkyo-ku, Tokyo 113-8655, Japan; [k]Department of Biochemistry and Molecular Biology, Bloomberg School of Public Health, The Johns Hopkins University, Baltimore, MD 21205; [l]National Center for Biotechnology Information, National Library of Medicine, National Institutes of Health, Bethesda, MD 20894; [n]Department of Biology and Biochemistry, University of Houston, Houston, TX 77204; and [o]RIKEN Preventive Medicine and Diagnosis Innovation Program, Wako, Saitama 351-0198, Japan

Edited by David P. Bartel, Massachusetts Institute of Technology, Cambridge, MA, and approved June 23, 2014 (received for review September 21, 2013)

Next-generation sequencing experiments have shown that microRNAs (miRNAs) are expressed in many different isoforms (isomiRs), whose biological relevance is often unclear. We found that mature miR-21, the most widely researched miRNA because of its importance in human disease, is produced in two prevalent isomiR forms that differ by 1 nt at their 3′ end, and moreover that the 3′ end of miR-21 is posttranscriptionally adenylated by the noncanonical poly(A) polymerase PAPD5. PAPD5 knockdown caused an increase in the miR-21 expression level, suggesting that PAPD5-mediated adenylation of miR-21 leads to its degradation. Exoribonuclease knockdown experiments followed by small-RNA sequencing suggested that PARN degrades miR-21 in the 3′-to-5′ direction. In accordance with this model, microarray expression profiling demonstrated that PAPD5 knockdown results in a down-regulation of miR-21 target mRNAs. We found that disruption of the miR-21 adenylation and degradation pathway is a general feature in tumors across a wide range of tissues, as evidenced by data from The Cancer Genome Atlas, as well as in the noncancerous proliferative disease psoriasis. We conclude that PAPD5 and PARN mediate degradation of oncogenic miRNA miR-21 through a tailing and trimming process, and that this pathway is disrupted in cancer and other proliferative diseases.

nucleotidyl transferase | microRNA processing

The advent and subsequently widespread use of next-generation sequencing technology has enabled the in-depth examination of the small RNA complement of cells. Among these small RNAs are microRNAs (miRNAs), a class of ∼22-nt RNAs that was discovered about 20 y ago (1). An impressive amount of miRNA sequencing data are now publicly available, which has aided the discovery of novel miRNAs, miRNA function, and miRNA biogenesis (2).

In the canonical miRNA generation pathway, RNA polymerase II or III produces the primary miRNA transcript from which the pre-miRNA hairpin is excised by DROSHA. The pre-miRNA is exported to the cytoplasm where it is cut by DICER1 to release a double-stranded RNA duplex consisting of the mature miRNA and the passenger strand. Whereas the passenger strand is usually rapidly degraded, the mature miRNA is loaded as a single-stranded RNA into an Argonaute protein to form the RNA-induced silencing complex (RISC) (3, 4). Within RISC the miRNA binds to partially complementary target sites in messenger RNAs, located preferentially in the 3′ UTR, to inhibit translation and induce degradation of the target mRNA. Base pairing to nucleotides to two to eight of the miRNA, the so-called seed sequence, is particularly important for target gene recognition.

In recent years, deep-sequencing libraries of small RNAs have revealed the existence of a large number of sequence variants both in pre-miRNAs and in mature miRNAs. In pre-miRNAs, sequence variations associated with adenosine-to-inosine (A-to-I) editing have been shown to affect their processing (5, 6). Similarly, polyuridylation mediated by the uridylyl transferase ZCCHC11 of the 3′ ends of pre-miRNAs of the let-7 miRNA family can suppress their maturation (7–10).

Significance

MicroRNAs (miRNAs) are small RNAs that regulate genes by selectively silencing their target messenger RNAs. They are often produced as various sequence variants that differ at their 3′ or 5′ ends. While 5′ sequence variations affect which messenger RNAs are targeted by the miRNA, the functional significance of 3′ sequence variants remains largely elusive. Here, we analyze 3′ sequence variants of miR-21, a miRNA well known for its crucial role in cancer and other diseases. We show that tumor suppressor PAPD5 mediates adenosine addition to the 3′ end of miR-21, followed by its 3′-to-5′ trimming by an exoribonuclease. We find that this degradation pathway is disrupted across a wide variety of cancers, highlighting its importance in human disease.

Author contributions: S.I., Y.H., and M.J.L.d.H. designed research; H.P., J.W.S., Y.I., I.S.N., R.S., K.I., K.-i.T., K.H.-I., Y.A., C. Sasaki, C. Suzuki, M.S., S.A., A.O., A.H., M.L., K.K., and C.R. performed research; J.B., C.C., and M.J.L.d.H. analyzed data; and J.B., H.P., S.M.H., A.M.B., B.T., P.C., H.S., P.H.G., C.R., and M.J.L.d.H. wrote the paper.

The authors declare no conflict of interest.

This article is a PNAS Direct Submission.

Data deposition: The sequences reported in this paper have been deposited in the DNA Data Bank of Japan Sequence Read Archive, http://trace.ddbj.nig.ac.jp/dra (accession nos. DRA002260–DRA002264, DRA002266, DRA002268, and DRA002269). The microarray data reported in this paper have been deposited in the Gene Expression Omnibus (GEO) database, www.ncbi.nlm.nih.gov/geo (accession no. GSE57939).

[1]Present address: Division of Oncology, Department of Clinical Sciences, Lund University Cancer Center/Medicon Village, SE-223 81 Lund, Sweden.

[2]To whom correspondence should be addressed. Email: mdehoon@gsc.riken.jp.

This article contains supporting information online at www.pnas.org/lookup/suppl/doi:10.1073/pnas.1317751111/-/DCSupplemental.

Sequence variations in mature miRNAs are referred to as isomiRs (11–13). IsomiRs may be produced by differential excision by DICER1, which can lead to variations in the 5′ and 3′ ends of the mature miRNA (14). This can alter their affinity for Argonaute proteins (15) and also, in case of 5′ end variations, their target specificity (16).

IsomiRs can also be generated by nontemplated addition of A and U nucleotides to their 3′ end (11, 17). Although several enzymes have been found to govern 3′ nucleotide addition to mature miRNAs (18), for most mature miRNAs 3′ adenylation is mediated by PAP associated domain containing 4 (PAPD4, also known as GLD2) (17). Whereas mature miR-122 is selectively stabilized by PAPD4-mediated adenylation (19), it remains unclear whether in general adenylation of the 3′ end of mature miRNAs increases their stability (17).

miRNAs are involved in the regulation of many cellular processes including developmental and oncogenic pathways (3, 20). The oncogenic miRNA (oncomiR) miR-21 (Fig. 1) has been of particular interest because of its importance in human diseases such as cancer (21–23), cardiovascular disease (22, 24), and inflammatory skin disease (25), with a role in cell cycle control (26), apoptosis (23), and metastasis (21, 27). Small-RNA sequencing data from The Cancer Genome Atlas (TCGA) (28) across a panel of 10 cancer types showed that miR-21 is the most highly expressed miRNA in cancer (Fig. S1*A*), with an expression level significantly elevated in tumor samples compared with the corresponding normal samples (Fig. S1*B*). Due to its biological and clinical importance, miR-21 is by far the most widely studied miRNA (Fig. S1*C*). Despite this, its isomiR composition and the functional significance of specific miR-21 isomiRs remain poorly understood.

Across a broad collection of small RNA deep-sequencing libraries, we found that two mature isomiRs of miR-21 are highly expressed, with their relative expression ratio strongly cell-type dependent. We show that the longer of the two isomiRs is the primary product of DICER1 cleavage, and that the shorter isomiR is produced by 3′-to-5′ degradation of miR-21 by a tailing-and-trimming process involving the nucleotidyl transferase PAP associated domain containing 5 (PAPD5) and the poly(A)-specific ribonuclease PARN. We then show that this degradation pathway is disrupted in most cancers, as well as in the noncancerous proliferative skin disease psoriasis. This provides evidence for a pathway in which PAPD5, a tumor suppressor previously shown to stabilize tumor protein p53 (TP53) mRNA (29), also regulates oncomiR degradation.

Results

miRNA-21 Has Two Prominent Isoforms. We produced a set of small-RNA libraries from MCF7 breast cancer cells (*SI Materials and Methods* and Fig. S2) and found that miR-21 accounted for more than 39% of total miRNA expression in this cell line (Fig. S3). Almost half of the overall miR-21 expression was due to a 23-nt isomiR, which we refer to as miR-21+C, that has an additional cytosine at the 3′ end compared with the 22-nt canonical miR-21 isomiR registered in miRBase (30) (Fig. 1 and Fig. S3). As this cytosine is encoded in the genome, miR-21+C may be produced directly by DICER1 processing of the pre–miR-21 hairpin structure. Reanalyzing small-RNA data previously produced at our laboratory from THP1 monocytic leukemia cells (31) revealed abundant expression of both isomiRs also in this cell line (Fig. S3). Previous Northern blotting experiments for miR-21 in RNA obtained from MCF7, HeLa, and HT29 cells (14) confirm the existence of both a 22-nt and a 23-nt mature miRNA in these cells.

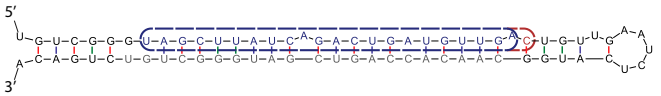

miR-21: UAGCUUAUCAGACUGAUGUUGA

miR-21+C: UAGCUUAUCAGACUGAUGUUGAC

miR-21+CA: UAGCUUAUCAGACUGAUGUUGACA

Passenger strand: CAACACCAGUCGAUGGGCUGU

$$\text{adenylation ratio} = \frac{\text{count of miR-21+CA}}{\text{count of miR-21+C}}$$

$$\text{degradation ratio} = \frac{\text{count of miR-21}}{\text{count of miR-21+C}}$$

Fig. 1. The upper image shows the structure of pre–miR-21 as predicted by mfold (55). The canonical miR-21 and miR-21+C isomiRs are highlighted in blue and burgundy, respectively. The definitions used in this paper appear below the structure.

miRNA-21+C Is the Primary Product of Pre–miR-21 Cleavage by DICER1. To understand the mechanism by which these two isomiRs are produced, we first considered the possibility that DICER1 itself is able to generate both isomiRs by alternative excision from the pre-miRNA hairpin. However, previously only a single 23-nt mature miRNA was observed after in vitro cleavage by DICER1 (32, 33), suggesting that at least in vitro DICER1 does not produce the 22-nt canonical miR-21 isomiR. Furthermore, although we would expect such alternative excision to be accompanied by a variation in the 5′ starting nucleotide of the miR-21 passenger strand sequence, we detected only a single dominant miR-21 passenger strand sequence both in our MCF7 as well as in our THP1 sequencing data (Fig. 1 and Fig. S4). Sequencing reads of the loop section of the pre–miR-21 hairpin structure are also consistent with excision by DICER1 of miR-21+C and do not show evidence of direct excision of the 22-nt canonical miR-21 isomiR (Fig. S4).

Association of human DICER1 with its partner protein TAR (HIV-1) RNA binding protein 2 (TARBP2, also known as TRBP) has previously been shown to alter its pre-miRNA cleavage pattern in vitro (32). However, Northern blots revealed only a single mature miRNA band of the same size after in vitro cleavage of pre–miR-21 by either DICER1 or the TARBP2–DICER1 complex (32), indicating that the existence of two distinct miR-21 isomiRs is not due to association of DICER1 with TARBP2.

Finally, we note that the 23-nt isomiR miR-21+C has a 2-nt overhang at its 3′ side with respect to the 5′ end of the passenger strand (Fig. 1 and Fig. S4), which is biochemically favorable and is typically seen in mature miRNA excision by DICER1 (34); in contrast, excision of the 22-nt canonical miR-21 isomiR would yield a single nucleotide overhang. We conclude that the miR-21+C isomiR is the primary product of DICER1 cleavage of pre–miR-21 both in vitro and in cell lines.

miRNA-21+C Is Subject to Cell-Type-Specific 3′ Adenylation. As DICER1 processing of pre–miR-21 only produces the 23-nt miR-21+C isomiR, we hypothesized that the canonical 22-nt mature miR-21 isomiR may instead be produced by 3′-to-5′ trimming of the 23-nt miR-21+C isomiR. Previously, stimulation of miR-21 degradation in HeLa cells by transfection of miR-21–specific antagomiRs was shown to not only result in 3′-to-5′ trimming of this miRNA, but also in its 3′ tailing by one or more nucleotides (35). In most cases, a single adenosine was added to the 3′ end of miR-21+C, giving rise to a 24-nt miR-21+CA isomiR. This adenosine is not encoded in the genome and is therefore likely to have been added posttranscriptionally to miR-21+C. In agreement with these previous results, we found that the miR-21+CA isomiR comprised between 1% and 10% of the miR-21 sequences in our MCF7 and THP1 sequencing data (Fig. S3).

To gauge whether these three isomiR forms are a general property of miR-21 expression in different cells and organisms, we examined publicly available sequencing datasets from human, rhesus macaque, mouse, rat, cow, platypus and Japanese flounder (Table S1). The examined data included both healthy and diseased samples, as well as primary tissue and cell lines, and between them cover ∼450 million y of evolution. Remarkably, miR-21, miR-21+C, and miR-21+CA were found in each of these datasets, with their abundances and relative counts varying between cell types (Fig. S3).

PAPD5 Adenylates the 3′ End of miR-21. Previously, we investigated nontemplated 3′ nucleotide additions to miRNAs by analyzing

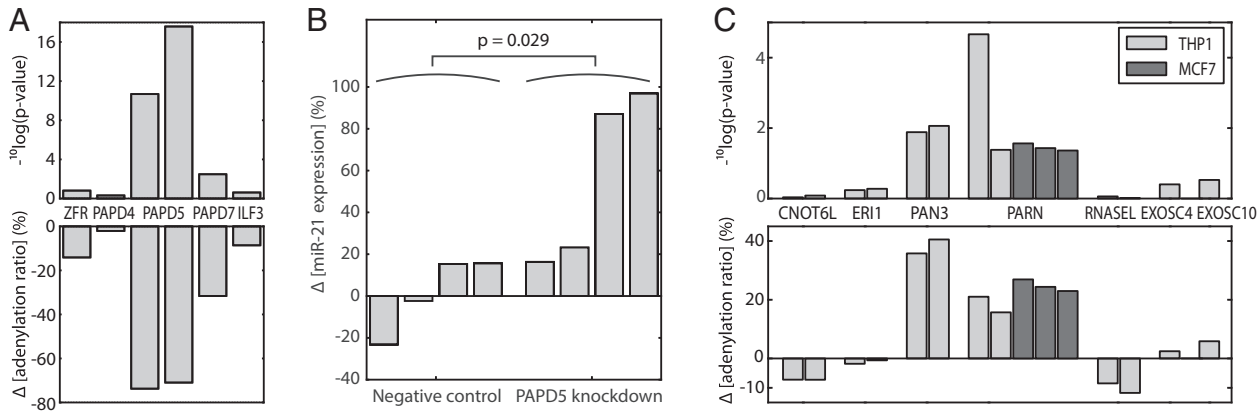

Fig. 2. (*A*) Deep-sequencing data of small RNAs from THP1 cells upon knockdown of candidate adenylating enzymes showed a large and highly significant decrease in the adenylation ratio of miR-21+C after knockdown of PAPD5, which was confirmed in a replicate PAPD5 knockdown experiment. (*B*) The expression level of miR-21, as measured by qPCR and normalized against the expression of the spliceosomal RNA U6, increased significantly upon knockdown of PAPD5 in THP1 cells. (*C*) Upon knockdown of exoribonuclease PARN, the miR-21+C adenylation ratio increased significantly compared with NC both in THP1 (two replicates) and in MCF7 (three replicates). In THP1, the miR-21+C adenylation ratio also increased significantly upon knockdown of PAN3.

sequencing data from THP1 cultures in which the nucleotidyl transferases ZFR, PAPD4, PAPD5, PAPD7, and ILF3 were knocked down by RNAi (17). We reanalyzed these data and found that knocking down PAPD5 dramatically decreases the adenylation ratio of miR-21+C (by 74%, P = 2.1e-11; Fig. 2*A*). This finding surprised us, as previously most miRNA 3′ adenylation events appeared to be mediated by PAPD4 and few, if any, by PAPD5 (17). We therefore repeated the PAPD5 knockdown experiment, which again showed a significant decrease in the miR-21+C adenylation ratio (by 71%; P = 2.6e-18; Fig. 2*A*). miR-142-3p was the only other miRNA that consistently showed a significant decrease in adenylation ratio in both replicates of the PAPD5 knockdown experiment (Fig. S5).

In vitro, PAPD5 has previously been shown to be an RNA-specific nucleotidyl transferase that can add adenosine to the 3′ end of a variety of oligoribonucleotides (36). To evaluate if also in cells PAPD5 acts directly on miR-21, we analyzed previously published photoactivatable-ribonucleoside-enhanced cross-linking and immunoprecipitation (PAR-CLIP) sequencing data obtained from HEK293 human embryonic kidney cells (36, 37). These data revealed a statistically significant fraction of miR-21 cross-linking to PAPD5 in two independent replicates (P = 3.7e-4 and P = 0.0072, respectively; *SI Materials and Methods* and Table S2), suggesting that the decrease in miR-21 adenylation observed in the PAPD5 knockdown libraries is a direct effect.

miRNA-21+C Is Trimmed at the 3′ End Following Its Adenylation. In human and murine liver cells, 3′ adenylation mediated by the nucleotidyl transferase PAPD4 has been shown to stabilize miR-122 (19). In contrast, PAPD5 was recently found to aid in the maturation of SNORA63 and other small nucleolar RNAs in a pathway where oligoadenylation by PAPD5 is followed by 3′-to-5′ trimming by the exonuclease PARN (38, 39) (Fig. S6). In all sequencing datasets shown in Fig. S3, we found miR-21+C transcripts with multiple adenosines added to their 3′ end. We hypothesized that miR-21+CA is similarly subject to 3′-to-5′ trimming, producing the 22-nt canonical miR-21 isomiR, which may subsequently be trimmed further in the 3′-to-5′ direction as part of a miR-21 degradation pathway. In all libraries, the vast majority of sequenced miR-21 reads shorter than the mature miRNA aligned to the 5′ end of miR-21, indicating that degradation of miR-21 indeed predominantly proceeds in the 3′-to-5′ direction. We regarded such 5′ matching reads shorter than 23 nt as putative miR-21 degradation products. In both PAPD5 knockdown libraries, we found a significant decrease in the counts of these degradation products compared with negative control (NC) (P = 1.2e-4 and P = 1.0e-5), suggesting that PAPD5-mediated adenylation of miR-21+C indeed promotes its 3′-to-5′ degradation (Fig. S7*A*). In agreement with such a degradation pathway, quantitative RT-PCR (qRT-PCR) showed a significantly higher expression level of miR-21 in THP1 cells upon PAPD5 knockdown compared with NC (P = 0.029; Fig. 2*B*).

To assess whether expression of PAPD5 is sufficient to stimulate adenylation and trimming of miR-21, we overexpressed the protein in THP1 and MCF7 cells using a lentiviral vector (*SI Materials and Methods* and Fig. S8*A*) and profiled their small RNAs by deep sequencing. Both in THP1 and in MCF7 cells, we found an increase in the abundance of miR-21 degradation products 2 wk post PAPD5 transduction compared with NC (Fig. S7 *B* and *C*). Confirming this observation we detected higher levels of miR-21 relative to miR-21+C (Fig. S7*D*). However, we failed to confirm the accumulation of degradation products using RNA samples extracted at an earlier time point posttransduction (Fig. S7*E*).

The Exoribonuclease PARN Mediates miR-21 Degradation. To identify the enzyme responsible for the 3′-to-5′ trimming of miR-21, we selected seven known exoribonucleases (CNOT6L, ERI1, PAN3 [poly(A) specific ribonuclease subunit], PARN, RNASEL,

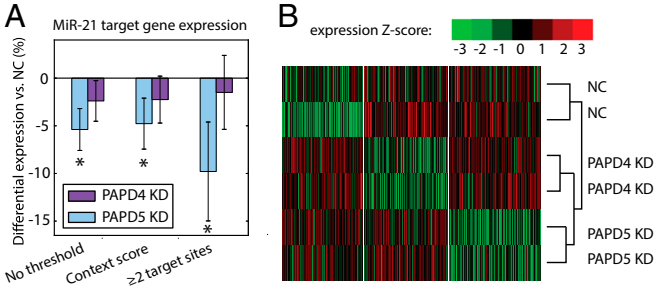

Fig. 3. Gene expression profiling in THP1 cells was performed using microarrays for two biological replicates each for the NC, the PAPD4 knockdown condition, and the PAPD5 knockdown condition. (*A*) Compared with NC, predicted target genes of miR-21 were significantly down-regulated upon knockdown of PAPD5, but not upon knockdown of PAPD4. This observation holds if more stringent selection criteria for miR-21 target genes are applied, such as requiring a context score lower than –0.2 or requiring multiple target sites for the same. Asterisks indicate statistically significant differential expression. Error bars represent the SDs of the estimated mean percentage change between the knockdown condition and the NC. (*B*) A heat map view of the expression data confirms that the profiled genes cluster by experimental condition.

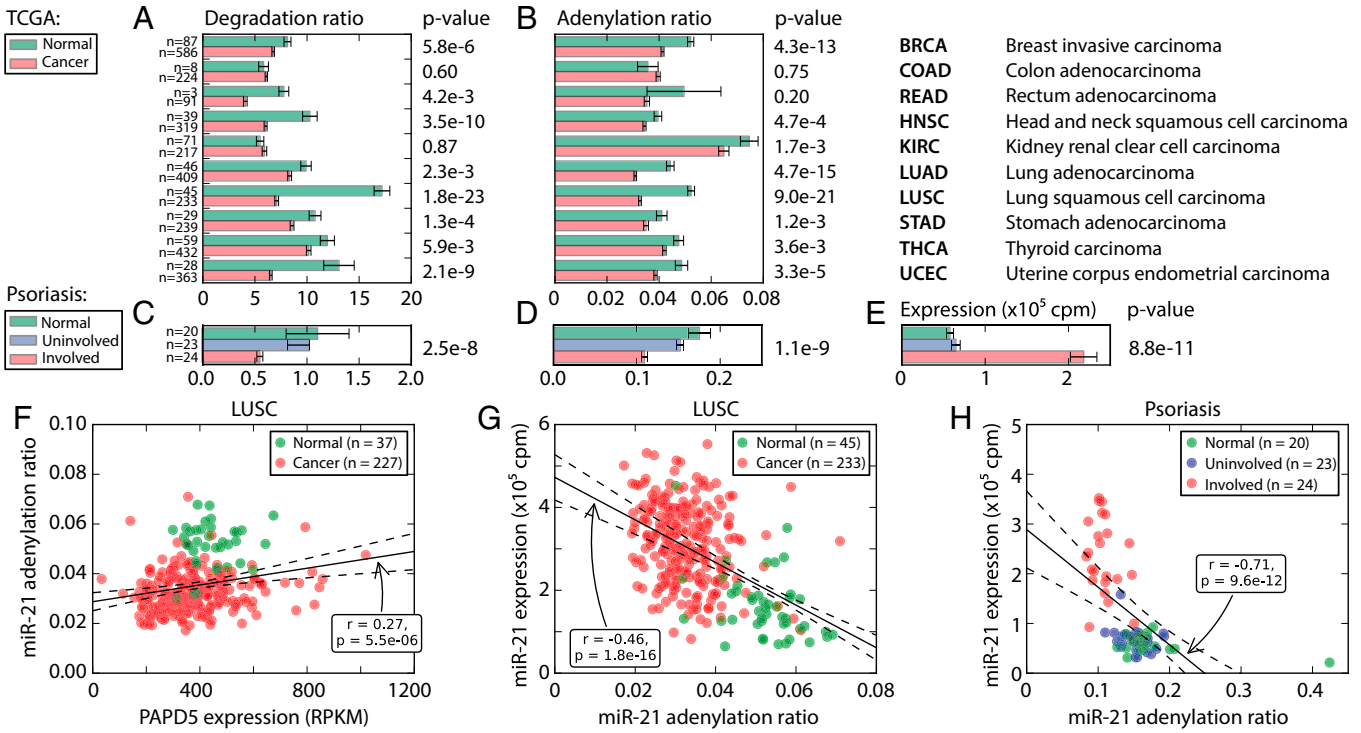

Fig. 4. Across a wide variety of cancers, the degradation ratio (*A*) and the adenylation ratio (*B*) of oncomir miR-21+C is significantly lower in tumor samples compared with normal samples. A reduced degradation ratio (*C*) and adenylation ratio (*D*) is also observed in psoriasis, which is similarly characterized by elevated expression levels of miR-21 (*E*). Error bars indicate the SD of the estimated mean; Kruskal–Wallis *P* values of the difference between healthy and disease samples are shown for each disease type. (*F*) As shown here for lung squamous cell carcinoma (LUSC), in most cancers the PAPD5 expression level is positively correlated with the miR-21 adenylation ratio, which in turn is negatively correlated with the miR-21 expression level (*G*). Similarly, in psoriasis the miR-21 adenylation ratio is negatively correlated with the miR-21 expression level (*H*). "Involved" refers to psoriatic skin samples, "uninvolved" to samples of skin from psoriatic patients that are not affected by psoriasis, and "normal" to skin from healthy donors. Dashed lines indicate the 95% confidence interval of the regression line. The Spearman correlation and its corresponding *P* value are shown. miRNA-21 expression levels are normalized to the overall miRNA expression level in each sample; PAPD5 expression levels are evaluated as reads per kilobase of transcript per million mapped reads (RPKMs). cpm, counts per million miRNAs.

EXOSC4, and EXOSC10), knocked down their expression in THP1 cells using RNAi (Fig. S8*B* and Table S3), and sequenced their small-RNA fraction. The sequencing data indeed revealed a significant increase in the adenylation ratio of miR-21+C upon PARN knockdown ($P = 2.2e\text{-}5$ and $P = 0.041$; Fig. 2*C*) as well as upon PAN3 knockdown ($P = 0.013$ and $P = 0.0086$; Fig. 2*C*).

Regarding the 3′-to-5′ trimming of miR-21 as a degradation process, we define the ratio of the miR-21 count to the miR-21+C count as the degradation ratio (Fig. 1). Although both replicates of the PARN knockdown showed a decrease in the degradation ratio (Fig. S7*F*), we did not observe a decrease of this ratio upon PAN3 knockdown in either replicate (Fig. S7*G*). This suggests that PARN, rather than PAN3, is the main exoribonuclease mediating 3′-to-5′ trimming and further degradation of miR-21. We further note that in both replicates of the PAN3 knockdown, on average, the adenylation ratio increased across all miRNAs ($P = 6.2e\text{-}4$ and $P = 1.6e\text{-}5$), suggesting that PAN3 acts as a deadenylating enzyme on a wide variety of miRNAs. No such effect was found for PARN, indicating that it acts specifically on miR-21.

To verify this role of PARN in a different cell type, we repeated its knockdown in MCF7 cells. Each of the three replicates again showed a significant increase in the miR-21 adenylation ratio ($P = 0.027$, $P = 0.037$, and $P = 0.043$; Fig. 2*C*), as well as a decrease in the degradation ratio (Fig. S7*H*).

PAPD5-Mediated Adenylation Affects Regulation by miR-21. To determine the downstream regulatory consequences of PAPD5-mediated adenylation and PARN-mediated degradation of miR-21+C, we analyzed gene expression in the PAPD4 and PAPD5 knockdown samples in THP1 cells using mRNA microarrays. Knockdown of PAPD4 and PAPD5 was confirmed both by qPCR and by the microarray expression profiling itself (Fig. S8 *C* and *D*). Target genes for miR-21 predicted by TargetScan (40, 41) showed significant down-regulation in the PAPD5 knockdown samples compared with the NC (Fig. 3*A*; $P = 0.002$). We also find a down-regulation of target genes upon PAPD5 knockdown if we restrict ourselves to confident target predictions by requiring a TargetScan context score lower than −0.2 (Fig. 3*A*; $P = 0.014$). In addition, the reduction in the expression of genes with at least two predicted miR-21 target sites was about twice as large compared with that of all predicted miR-21 target genes (Fig. 3*A*; $P = 0.029$). None of these sets of genes showed a statistically significant down-regulation upon PAPD4 knockdown, demonstrating that the effect on miR-21 target genes is specific for PAPD5. Hierarchical clustering of the microarray expression data with respect to the knockdown conditions reveals distinct clustering into an NC cluster, a PAPD4 knockdown cluster, and a PAPD5 knockdown cluster (Fig. 3*B*).

Dysregulation of the miR-21 Degradation Pathway in Proliferative Disease. To evaluate the relevance of the miR-21 degradation pathway in disease, we analyzed RNA sequencing and small-RNA sequencing data from clinical samples from TCGA (28). We applied our analysis to the 10 cancer types for which the TCGA data are currently publicly available, and for which both tumor and normal samples have been profiled (Fig. 4). Across most cancer types, both the miR-21 degradation ratio (Fig. 4*A*) and the miR-21 adenylation ratio (Fig. 4*B*) were significantly

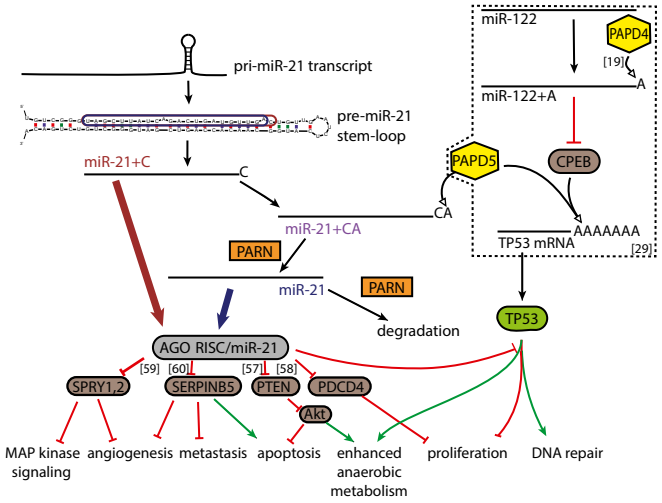

Fig. 5. PAPD5 prolongs the life of the mRNA encoding tumor suppressor TP53 by polyadenylation. By adenylating miR-21+C and thus inducing its degradation by PARN, PAPD5 prevents the oncomiR from repressing other tumor suppressors. Once associated with an Argonaute protein, miR-21 isomiRs engage in the promotion of a variety of classical cancer hallmarks (56), such as angiogenesis, the avoidance of apoptosis, altered signaling, metastasis, enhanced anaerobic metabolism, and enhanced proliferation. The miR-21 targets shown in this figure have all been experimentally verified [PTEN (57), PDCD4 (58), SPRY1 (59), and SERPINB5 (60)]. Nucleotidyl transferases are represented as yellow hexagons; TP53, a key transcription factor involved in tumor suppression, is represented by a green rounded rectangle; the exoribonuclease PARN is shown in orange; and regulatory interactions are represented by green arrows (up-regulation or stimulation) or red "inhibition" arrows (down-regulation or inhibition). The uptake of canonical miR-21 and miR-21+C into the RISC complex is denoted by arrows. Adenylated miR-21+C undergoes degradation by the 3′ exoribonuclease PARN, which yields the 22 nt miR-21 and shorter degradation products.

lower in the tumor samples compared with the corresponding normal samples; there were no significantly elevated degradation ratios or adenylation ratios in any of the cancer types. Consistent with PAPD5-mediated adenylation of miR-21 leading to its degradation, across most cancer types we found a statistically significant positive correlation between PAPD5 expression level and adenylation ratio (Fig. 4*F* and Fig. S9*A*), and a significant negative correlation between the adenylation ratio of miR-21 and its expression level (Fig. 4*G* and Fig. S9*B*). The remaining correlation values were not significantly different from zero. Combined, the above indicates that disruptions in the degradation pathway of miR-21 are a hallmark of cancer across a wide range of tissues.

We then asked whether disruption of the miR-21 degradation pathway is relevant in noncancerous proliferative diseases such as psoriasis, a skin disease characterized by increased proliferation of basal cells in the epidermis (42). Small RNA-sequencing data consisting of 67 patient samples of psoriatic and normal skin previously revealed (25) that at the molecular level psoriasis, like cancer, is characterized by elevated expression levels of miR-21 (Kruskal–Wallis P = 8.8e-11; Fig. 4*E*). Analyzing the miR-21 isomiR counts across these samples showed that the adenylation ratio is negatively correlated with the miR-21 expression level (r = –0.71; P = 9.6e-12; Fig. 4*H*), with the miR-21+C degradation ratio and adenylation ratio significantly lower in psoriasis samples compared with unaffected skin (Kruskal–Wallis P = 2.5e-8 and P = 1.1e-9, respectively; Fig. 4 *C* and *D*). Hence, we conclude that dysregulation of the miR-21 degradation pathway is not limited to cancer, but can also occur in other types of proliferative disease.

Discussion

In recent years, several posttranscriptional mechanisms have been uncovered that enable the fine-grained regulation of individual miRNAs beyond the canonical maturation pathway (3, 43, 44). Next-generation sequencing of miRNAs has revealed a wide variety of miRNA variants that may be produced by differential excision by DICER1 or nucleotide additions to the 3′ ends of miRNAs or their precursors (11, 45). Multiple nucleotidyl transferases, including PAPD4 and PAPD5, can mediate 3′ adenylation of mature miRNAs in human (17, 18); these 3′ additions have been shown to be a physiological phenomenon rather than an artifact of library preparation and are specific for different miRNAs (18). However, the biogenesis and biological significance of miRNA 3′ modifications as well as isomiRs with distinct 3′ ends are generally poorly understood.

Whereas mature miRNAs generally are stable and tend to persist even if the processing enzymes are depleted by RNAi (46, 47), examples are known in which specific miRNAs are degraded rapidly (48), and sequence-specific tailing and trimming was recently reported as a mechanism of miR-27a/b depletion in mouse (49). Our results show that 3′ adenylation of oncomiR miR-21 by the nucleotidyl transferase PAPD5 may similarly lead to its degradation by targeting it for 3′ end trimming by exoribonuclease PARN. This enzyme thus is a human ortholog of the exonuclease Nibbler, which was recently discovered to trim the 3′ ends of miRNAs in *Drosophila* (43, 44). PARN was recently also shown to trim the 3′ arm of human pre–miR-451 in the 3′-to-5′ direction as the final step in the maturation pathway of this miRNA (50).

In liver cells, an additional biological function of PAPD5 was recently discovered in a regulatory pathway affecting the tumor suppressor TP53 (also known as p53) (29). In this pathway, PAPD4 stabilizes the miRNA miR-122 by 3′ adenylation (19), thereby stimulating translational repression by miR-122 of the cytoplasmic polyadenylation element-binding protein CPEB. This protein binds to the 3′ UTR of TP53 mRNA and recruits PAPD5, which modulates the stability and translation of the TP53 mRNA by polyadenylating its 3′ end. Hence, PAPD5 acts as a tumor suppressor by regulating translation of TP53 and thus promoting cellular senescence (Fig. 5) (29). Interestingly, PARN was recently shown to trim polyadenylated TP53 mRNA (51), which suggests a combined role for PAPD5 and PARN both in the regulation of TP53 abundance and in regulation of miR-21 after DICER1 cleavage.

Enzymatic addition of adenosine or uracil nucleotides to the 3′ end of miRNAs may in general modulate their stability and thereby play a role in regulating their abundance (20). Whereas miR-122 was previously shown to be stabilized by PAPD4-mediated adenylation of its 3′ end (19, 20), we find instead that 3′ terminal addition by PAPD5 to miR-21 stimulates its degradation. This suggests the existence of a regulatory network of 3′ nucleotidyl transferases and exoribonucleases targeting specific mature miRNAs to enhance or prevent their degradation. As evidenced by our analysis of small RNA-sequencing data from clinical samples, the degradation pathway of miR-21 we identified is frequently disrupted across a wide variety of proliferative diseases, underscoring the importance of this regulatory network in human health and disease.

Materials and Methods

A detailed description of the materials, data sources, and experimental and analysis methods is provided in *SI Materials and Methods*.

Analysis of miR-21 Isoforms in Sequencing Data. For human, the mature miR-21 sequence listed in miRBase (30) is the common 22-nt isoform UAGCUUAUCAGACUGAUGUUGA. This 22-nt sequence and its 3′ downstream sequence are conserved in all species we analyzed, except for Japanese flounder (52), for which the mature sequence is UAGCUUAUCAGACUGGUGUUGG but the downstream sequence is the same as for the other species.

Statistical Analysis of Adenylation/Degradation Ratios and Overrepresentation of Degradation Products. The enzyme knockdown conditions were analyzed separately by comparing the sequence counts for isomiRs in the knockdown condition to their sequence counts in the NC to estimate the common dispersion of the negative binomial distribution (53) using the maximum likelihood method. We then used the likelihood ratio test (54) to calculate the statistical significance of differences in adenylation ratios between each knockdown condition and the NC for each miRNA.

ACKNOWLEDGMENTS. The authors thank Fumi Hori for technical assistance, and Noriko Nakanishi for technical assistance and help with the manuscript. The authors also thank The Institute of Physical and Chemical Research (RIKEN) Genome Network Analysis Support Facility for the sequencing of the MCF7 small-RNA libraries using an Illumina Genome Analyzer, and of the THP1 and MCF7 libraries on an Illumina HiSeq 2000. Additionally the authors thank the The Cancer Genome Atlas (TCGA) Research Network for providing access to the data of TCGA. This work was supported by a research grant for RIKEN Omics Science Centre (which ceased to exist as of April 1, 2013, due to RIKEN reorganization) from Ministry of Education, Culture, Sports, Science and Technology (MEXT) (to Y.H.); a grant of the Genome Network Project from MEXT (to Y.H.); a grant of the Innovative Cell Biology by Innovative Technology (Cell Innovation Program) from MEXT (to Y.H.); a research grant from MEXT to the RIKEN Center for Life Science Technologies; a research grant from MEXT (to the RIKEN Preventive Medicine and Diagnosis Innovation Program); a grant from the Hendrik Muller Foundation (Netherlands) (to J.B.); a grant from the Eunice Kennedy Shriver National Institute of Child Health and Human Development/National Institutes of Health through Cooperative Agreements U54HD007495 (to S.M.H.); and a grant from the Japan Society for the Promotion of Science (to M.J.L.d.H.).

1. Lee RC, Feinbaum RL, Ambros V (1993) The C. elegans heterochronic gene lin-4 encodes small RNAs with antisense complementarity to lin-14. *Cell* 75(5):843–854.
2. Lee LW, et al. (2010) Complexity of the microRNA repertoire revealed by next-generation sequencing. *RNA* 16(11):2170–2180.
3. Winter J, Jung S, Keller S, Gregory RI, Diederichs S (2009) Many roads to maturity: MicroRNA biogenesis pathways and their regulation. *Nat Cell Biol* 11(3):228–234.
4. Hutvagner G, Simard MJ (2008) Argonaute proteins: Key players in RNA silencing. *Nat Rev Mol Cell Biol* 9(1):22–32.
5. Kawahara Y, Zinshteyn B, Chendrimada TP, Shiekhattar R, Nishikura K (2007) RNA editing of the microRNA-151 precursor blocks cleavage by the Dicer-TRBP complex. *EMBO Rep* 8(8):763–769.
6. Kawahara Y, et al. (2008) Frequency and fate of microRNA editing in human brain. *Nucleic Acids Res* 36(16):5270–5280.
7. Viswanathan SR, Daley GQ, Gregory RI (2008) Selective blockade of microRNA processing by Lin28. *Science* 320(5872):97–100.
8. Heo I, et al. (2008) Lin28 mediates the terminal uridylation of let-7 precursor MicroRNA. *Mol Cell* 32(2):276–284.
9. Heo I, et al. (2009) TUT4 in concert with Lin28 suppresses microRNA biogenesis through pre-microRNA uridylation. *Cell* 138(4):696–708.
10. Hagan JP, Piskounova E, Gregory RI (2009) Lin28 recruits the TUTase Zcchc11 to inhibit let-7 maturation in mouse embryonic stem cells. *Nat Struct Mol Biol* 16(10):1021–1025.
11. Landgraf P, et al. (2007) A mammalian microRNA expression atlas based on small RNA library sequencing. *Cell* 129(7):1401–1414.
12. Kuchenbauer F, et al. (2008) In-depth characterization of the microRNA transcriptome in a leukemia progression model. *Genome Res* 18(11):1787–1797.
13. Morin RD, et al. (2008) Application of massively parallel sequencing to microRNA profiling and discovery in human embryonic stem cells. *Genome Res* 18(4):610–621.
14. Starega-Roslan J, et al. (2011) Structural basis of microRNA length variety. *Nucleic Acids Res* 39(1):257–268.
15. Burroughs AM, et al. (2011) Deep-sequencing of human Argonaute-associated small RNAs provides insight into miRNA sorting and reveals Argonaute association with RNA fragments of diverse origin. *RNA Biol* 8(1):158–177.
16. Azuma-Mukai A, et al. (2008) Characterization of endogenous human Argonautes and their miRNA partners in RNA silencing. *Proc Natl Acad Sci USA* 105(23):7964–7969.
17. Burroughs AM, et al. (2010) A comprehensive survey of 3′ animal miRNA modification events and a possible role for 3′ adenylation in modulating miRNA targeting effectiveness. *Genome Res* 20(10):1398–1410.
18. Wyman SK, et al. (2011) Post-transcriptional generation of miRNA variants by multiple nucleotidyl transferases contributes to miRNA transcriptome complexity. *Genome Res* 21(9):1450–1461.
19. Katoh T, et al. (2009) Selective stabilization of mammalian microRNAs by 3′ adenylation mediated by the cytoplasmic poly(A) polymerase GLD-2. *Genes Dev* 23(4): 433–438.
20. Krol J, Loedige I, Filipowicz W (2010) The widespread regulation of microRNA biogenesis, function and decay. *Nat Rev Genet* 11(9):597–610.
21. Yang CH, Yue J, Pfeffer SR, Handorf CR, Pfeffer LM (2011) MicroRNA miR-21 regulates the metastatic behavior of B16 melanoma cells. *J Biol Chem* 286(45):39172–39178.
22. Jazbutyte V, Thum T (2010) MicroRNA-21: From cancer to cardiovascular disease. *Curr Drug Targets* 11(8):926–935.
23. Medina PP, Nolde M, Slack FJ (2010) OncomiR addiction in an in vivo model of microRNA-21-induced pre-B-cell lymphoma. *Nature* 467(7311):86–90.
24. Cheng Y, Zhang C (2010) MicroRNA-21 in cardiovascular disease. *J Cardiovasc Transl Res* 3(3):251–255.
25. Joyce CE, et al. (2011) Deep sequencing of small RNAs from human skin reveals major alterations in the psoriasis miRNAome. *Hum Mol Genet* 20(20):4025–4040.
26. Liu M, et al. (2009) Regulation of the cell cycle gene, BTG2, by miR-21 in human laryngeal carcinoma. *Cell Res* 19(7):828–837.
27. Niu J, et al. (2012) DNA damage induces NF-κB-dependent microRNA-21 up-regulation and promotes breast cancer cell invasion. *J Biol Chem* 287(26):21783–21795.
28. The Cancer Genome Atlas. Available at http://cancergenome.nih.gov. Accessed August 29, 2013.
29. Burns DM, D'Ambrogio A, Nottrott S, Richter JD (2011) CPEB and two poly(A) polymerases control miR-122 stability and p53 mRNA translation. *Nature* 473(7345): 105–108.
30. Kozomara A, Griffiths-Jones S (2014) miRBase: Annotating high confidence microRNAs using deep sequencing data. *Nucleic Acids Res* 42(Database issue):D68–D73.
31. Taft RJ, et al. (2009) Tiny RNAs associated with transcription start sites in animals. *Nat Genet* 41(5):572–578.
32. Lee HY, Doudna JA (2012) TRBP alters human precursor microRNA processing in vitro. *RNA* 18(11):2012–2019.
33. Ando Y, et al. (2011) Two-step cleavage of hairpin RNA with 5′ overhangs by human DICER. *BMC Mol Biol* 12:6.
34. Zhang H, Kolb FA, Jaskiewicz L, Westhof E, Filipowicz W (2004) Single processing center models for human Dicer and bacterial RNase III. *Cell* 118(1):57–68.
35. Ameres SL, et al. (2010) Target RNA-directed trimming and tailing of small silencing RNAs. *Science* 328(5985):1534–1539.
36. Rammelt C, Bilen B, Zavolan M, Keller W (2011) PAPD5, a noncanonical poly(A) polymerase with an unusual RNA-binding motif. *RNA* 17(9):1737–1746.
37. Hafner M, et al. (2010) Transcriptome-wide identification of RNA-binding protein and microRNA target sites by PAR-CLIP. *Cell* 141(1):129–141.
38. Berndt H, et al. (2012) Maturation of mammalian H/ACA box snoRNAs: PAPD5-dependent adenylation and PARN-dependent trimming. *RNA* 18(5):958–972.
39. Virtanen A, Henriksson N, Nilsson P, Nissbeck M (2013) Poly(A)-specific ribonuclease (PARN): An allosterically regulated, processive and mRNA cap-interacting deadenylase. *Crit Rev Biochem Mol Biol* 48(2):192–209.
40. Friedman RC, Farh KK, Burge CB, Bartel DP (2009) Most mammalian mRNAs are conserved targets of microRNAs. *Genome Res* 19(1):92–105.
41. Lewis BP, Shih IH, Jones-Rhoades MW, Bartel DP, Burge CB (2003) Prediction of mammalian microRNA targets. *Cell* 115(7):787–798.
42. Roberson ED, Bowcock AM (2010) Psoriasis genetics: Breaking the barrier. *Trends Genet* 26(9):415–423.
43. Liu N, et al. (2011) The exoribonuclease Nibbler controls 3′ end processing of microRNAs in Drosophila. *Curr Biol* 21(22):1888–1893.
44. Han BW, Hung JH, Weng Z, Zamore PD, Ameres SL (2011) The 3′-to-5′ exoribonuclease Nibbler shapes the 3′ ends of microRNAs bound to Drosophila Argonaute1. *Curr Biol* 21(22):1878–1887.
45. Burroughs AM, Kawano M, Ando Y, Daub CO, Hayashizaki Y (2012) pre-miRNA profiles obtained through application of locked nucleic acids and deep sequencing reveals complex 5′/3′ arm variation including concomitant cleavage and polyuridylation patterns. *Nucleic Acids Res* 40(4):1424–1437.
46. Lee Y, et al. (2003) The nuclear RNase III Drosha initiates microRNA processing. *Nature* 425(6956):415–419.
47. Gregory RI, et al. (2004) The microprocessor complex mediates the genesis of microRNAs. *Nature* 432(7014):235–240.
48. Pedersen IM, et al. (2007) Interferon modulation of cellular microRNAs as an antiviral mechanism. *Nature* 449(7164):919–922.
49. Marcinowski L, et al. (2012) Degradation of cellular mir-27 by a novel, highly abundant viral transcript is important for efficient virus replication in vivo. *PLoS Pathog* 8(2):e1002510.
50. Yoda M, et al. (2013) Poly(A)-specific ribonuclease mediates 3′-end trimming of Argonaute2-cleaved precursor microRNAs. *Cell Reports* 5(3):715–726.
51. Devany E, Zhang X, Park JY, Tian B, Kleiman FE (2013) Positive and negative feedback loops in the p53 and mRNA 3′ processing pathways. *Proc Natl Acad Sci USA* 110(9): 3351–3356.
52. Fu Y, et al. (2011) Identification and differential expression of microRNAs during metamorphosis of the Japanese flounder (Paralichthys olivaceus). *PLoS ONE* 6(7): e22957.
53. Robinson MD, McCarthy DJ, Smyth GK (2010) edgeR: A Bioconductor package for differential expression analysis of digital gene expression data. *Bioinformatics* 26(1): 139–140.
54. Wilks SS (1938) The large-sample distribution of the likelihood ratio for testing composite hypotheses. *Ann Math Stat* 9(1):60–62.
55. Zuker M (2003) Mfold web server for nucleic acid folding and hybridization prediction. *Nucleic Acids Res* 31(13):3406–3415.
56. Hanahan D, Weinberg RA (2011) Hallmarks of cancer: The next generation. *Cell* 144(5):646–674.
57. Meng F, et al. (2007) MicroRNA-21 regulates expression of the PTEN tumor suppressor gene in human hepatocellular cancer. *Gastroenterology* 133(2):647–658.
58. Asangani IA, et al. (2008) MicroRNA-21 (miR-21) post-transcriptionally downregulates tumor suppressor Pdcd4 and stimulates invasion, intravasation and metastasis in colorectal cancer. *Oncogene* 27(15):2128–2136.
59. Thum T, et al. (2008) MicroRNA-21 contributes to myocardial disease by stimulating MAP kinase signalling in fibroblasts. *Nature* 456(7224):980–984.
60. Zhu S, et al. (2008) MicroRNA-21 targets tumor suppressor genes in invasion and metastasis. *Cell Res* 18(3):350–359.